Chemistry–A European Journal

Supporting Information

Unveiling Luminescent Ir^{I} and Rh^{I} N-Heterocyclic Carbene Complexes: Structure, Photophysical Specifics, and Cellular Localization in the Endoplasmic Reticulum

Isabelle Marie Daubit,[a] Svenja Wortmann,[b] Daniel Siegmund,[c] Stephan Hahn,[d] Patrick Nuernberger,[b] and Nils Metzler-Nolte*[a]

Content

1. General experimental information

1.1 Technical equipment and procedures

1.1.1 Chromatographic purifications

Normal phase chromatographic purification of the crude products was carried out either by normal phase column chromatography on silica gel purchased from Macherey Nagel with a particle size of 60 Å or with the Combi Flash Rf chromatography system with Chromabond SiOH columns purchased from Macherey Nagel by solid load technique.

1.1.2 Nuclear magnetic resonance

All samples for nuclear magnetic resonance analysis were prepared with deuterated solvents from commercial suppliers, which were also used as internal reference. The chemical shift δ is given in ppm relative to TMS. ^{1}H-NMR and ^{13}C-NMR were recorded with either one of the following spectrometers: Bruker Advance DPX-200 (^{1}H: 200 MHz, ^{13}C: 50 MHz), Bruker DPX-250 (^{1}H: 250 MHz, ^{13}C: 62.9 MHz), Bruker AV III 300 Nanobay (^{1}H: 300 MHz, ^{13}C: 75 MHz), AV III 400 HD (^{1}H: 400 MHz, ^{13}C: 101 MHz) or Bruker DRX 400 (^{1}H: 400 MHz, ^{13}C: 101 MHz). Data were obtained from the instrument and processed with MestreNova Version 10.0.2.

1.1.3 Mass spectrometry

ESI mass spectra were recorded on a Bruker Esquire 6000 using LC-MS grade methanol or acetonitrile for sample preparation. The samples were filtered through a 0.2 µm syringe filter prior use and entered the device without air bubbles. Data were obtained from the instrument, processed with DataAnalysis from Bruker, exported as simple x,y files and processed with Excel 2010.

1.1.4 Calculation of PCC values

Confocal microscopy has been performed in the Department of Medicine (Anatomy and Molecular Embryology) at the Ruhr University Bochum with the permission of Prof. Dr. Brand-Saberi under guidance of Dr. Nenad Maricic and Britta Redeker. The initial raw pictures were processed with Zen 3.0 blue edition from Zeiss. Pictures suitable for the determination of PCC values were exported and processed with ImageJ to obtain the blue and red pixel values. These raw data were exported as x,y files and further processed with Excel 2010. PCC values were then calculated according to the following equation, where R represents the red pixel intensity while B represents the blue pixel intensity:

$$PCC = \frac{\sum_i \left(R_i - \bar{R}\right) \times \left(B_i - \bar{B}\right)}{\sqrt{\sum_i (R_i - \bar{R})^2 \times \sum_i (B_i - \bar{B})^2}}$$

2. Supplementary Figures

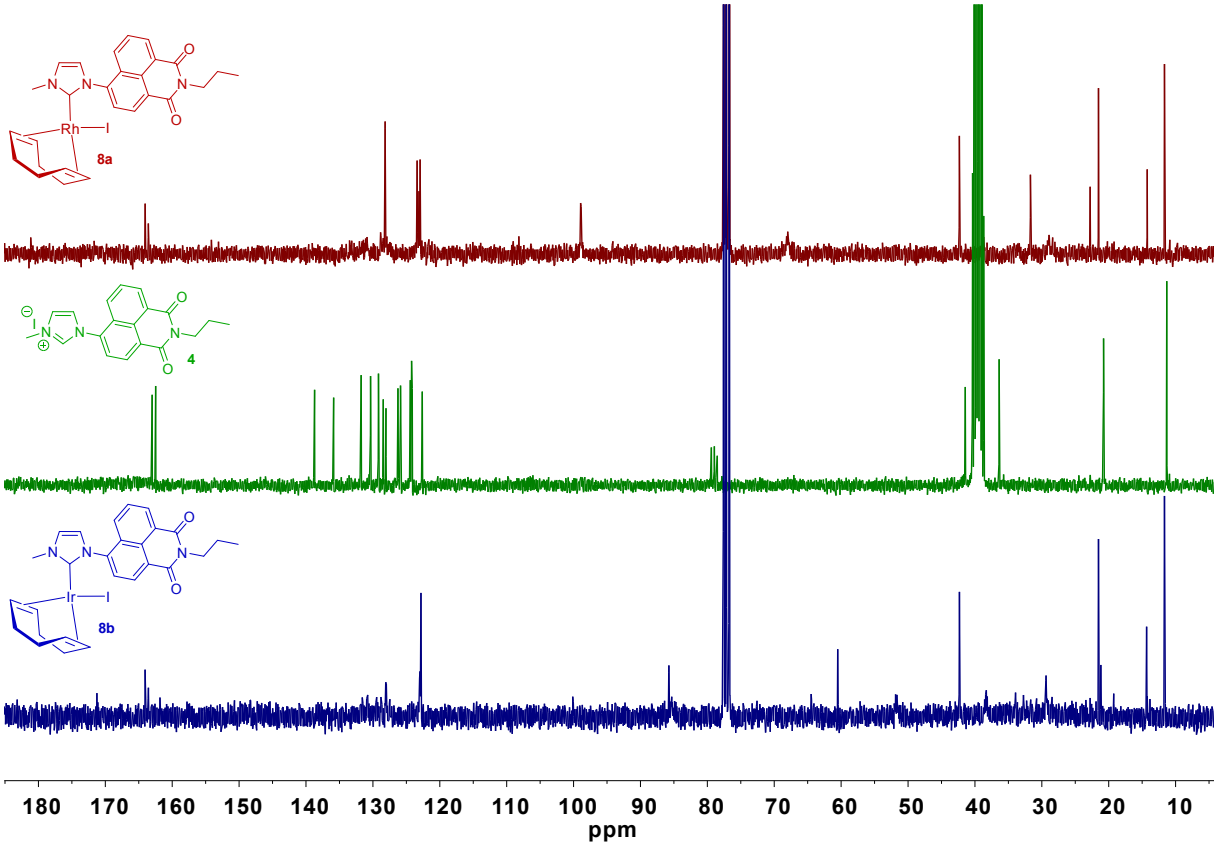

Figure S1. *^{13}C-NMR spectra of rhodium complex **8a** (upper, red trace, 200 MHz in $CDCl_3$), 1,8naphtalimide derivative **4** (middle, green trace, 200 MHz in DMSO-d_6) and iridium complex **8b** (lower, blue trace, 200 MHz in $CDCl_3$) recorded at ambient temperature. The upper and lower trace show only very few signals in the aromatic area of the spectrum between 140 ppm and 120 ppm where several more signals would be expected with respect to the spectrum of the free ligand in the middle.*

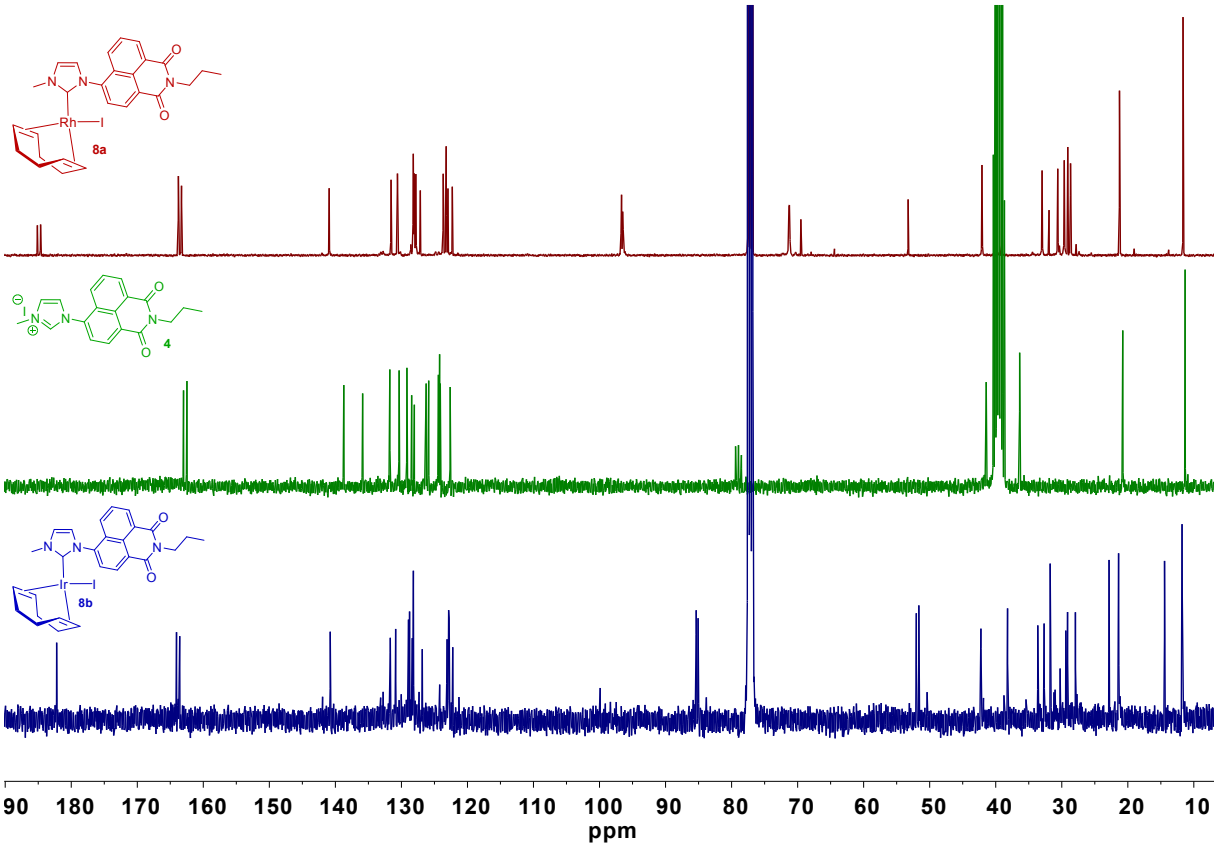

Figure S2. *^{13}C-NMR spectra of rhodium complex **8a** (upper, red trace, 400 MHz in $CDCl_3$), 1,8naphtalimide derivative **4** (middle, green trace, 200 MHz in DMSO-d_6) and iridium complex **8b** (lower, blue trace, 400 MHz in $CDCl_3$) recorded at -30°C. In comparison to the spectra recorded at ambient temperature, the upper and lower trace now show the peaks in the aromatic area of the spectrum between 140 ppm and 120 ppm which are expected from the spectrum of the free ligand in the middle.*

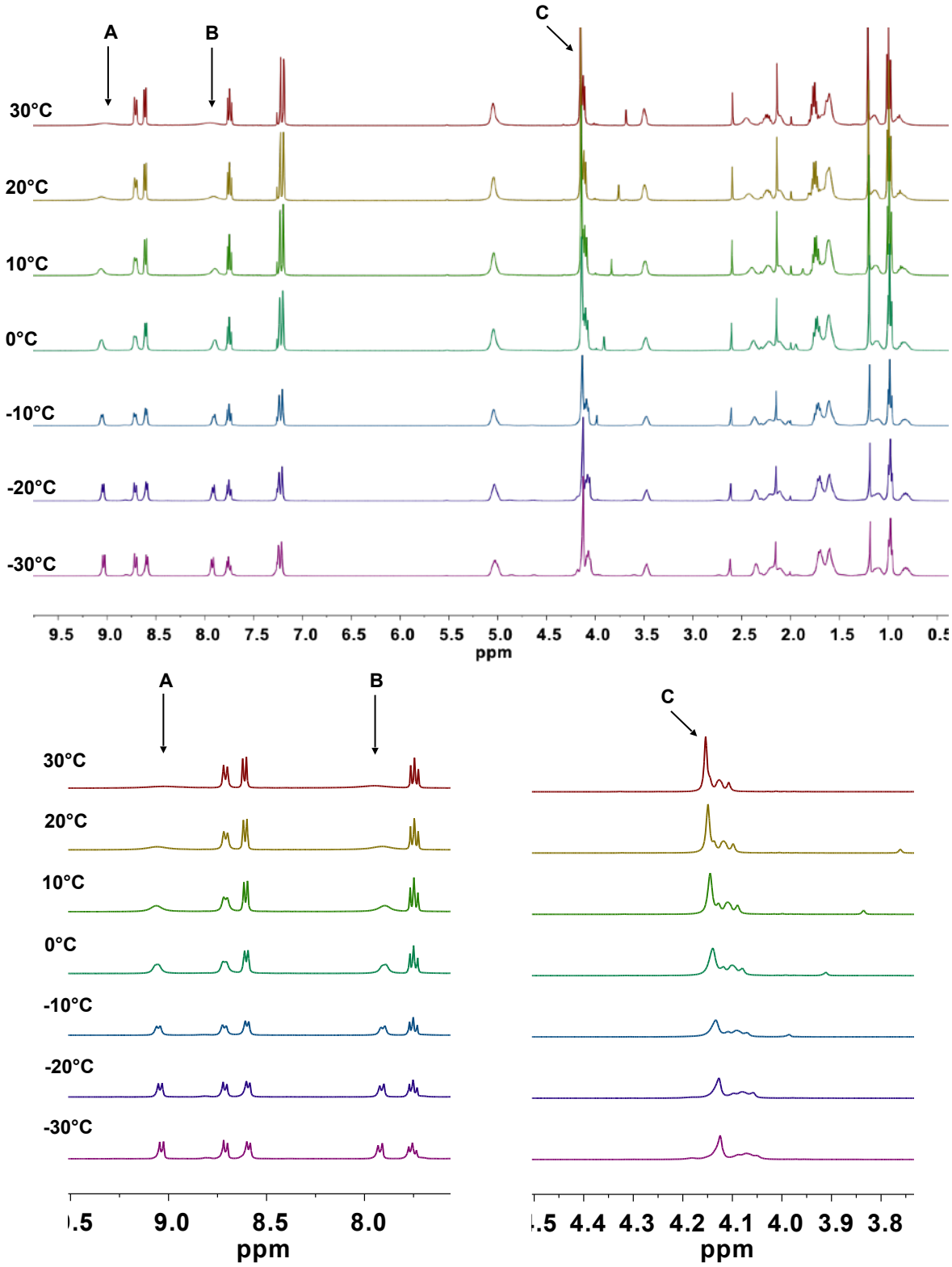

Figure S3. *Upper part: Temperature dependent ^{1}H-NMR spectra (400 MHz in $CDCl_3$) recorded from 30°C to -30°C of complex **8a**. The signals A and B (aromatic protons, marked with an arrow) change their shape from a very broad signal to a sharp doublet. Lower, left part: Zoom into the area from 10 ppm to 7.5 ppm showing the temperature dependent development of signals A and B in detail. Lower, right part: Zoom of the area between 4.5 ppm and 3.7 ppm showing the signal of the imidazolium methyl group (signal C) showing no change in signal shape.*

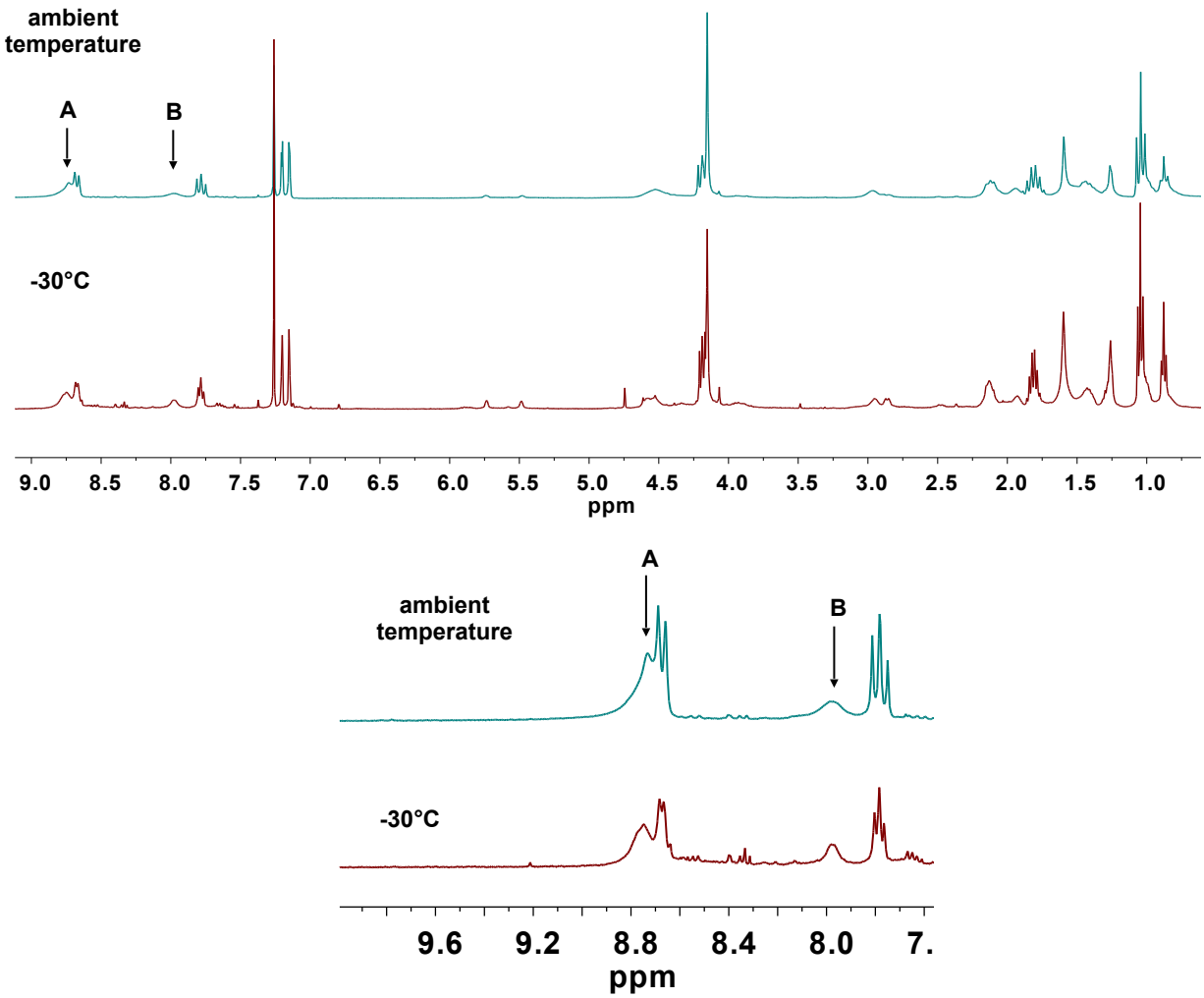

Figure S4. *Upper part: ^{1}H-NMR spectrum of complex* ***9b*** *at ambient temperature (upper, green trace, 200 MHz in $CDCl_3$) and at -30°C (lower, red trace, 400 MHz in $CDCl_3$). The signals A and B (aromatic protons, marked with an arrow) show a slight change in signal shape when the sample is cooled down. Lower part: Zoom into the area between 7.9 ppm and 9.8 ppm showing the change in signal shape for signals A and B in more detail.*

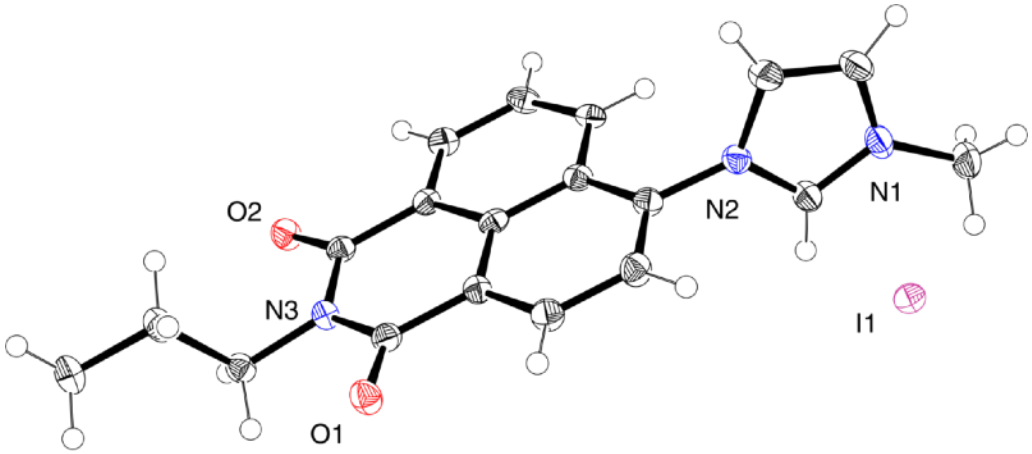

Figure S5. *X-Ray crystal structure of ligand* ***4*** *(ellipsoid probability 30%).*

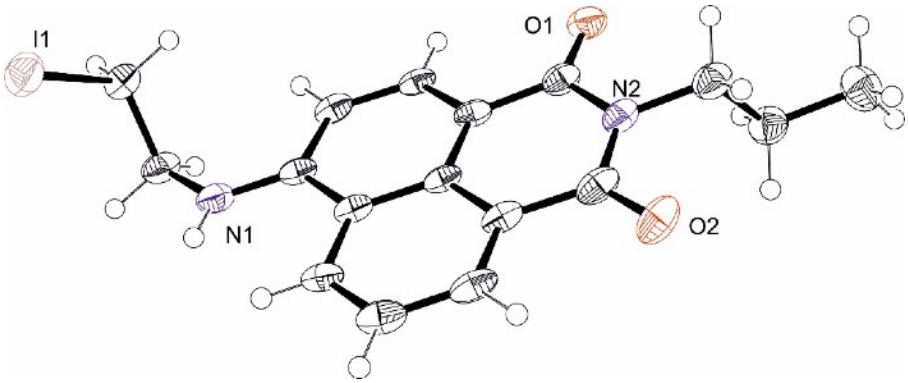

Figure S6. *X-Ray crystal structure of compound* ***6*** *(ellipsoid probability 30%).*

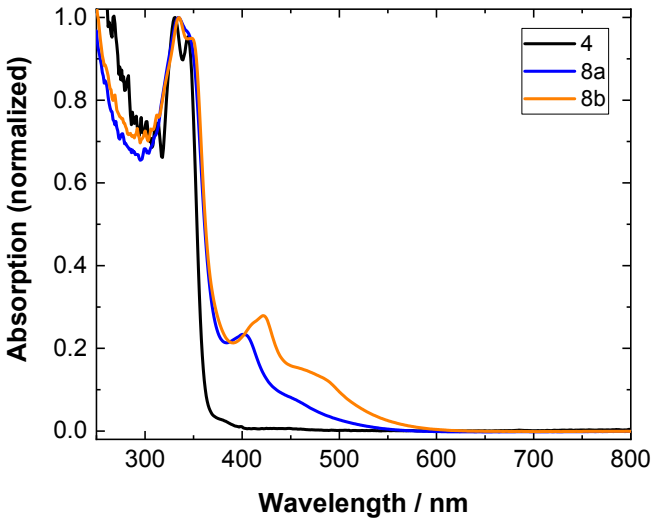

Figure S7. *Steady-state UV/Vis absorption spectra of the complexes* ***8a*** *(blue),* ***8b*** *(orange) and the free NHC ligand (black) recorded in acetone.*

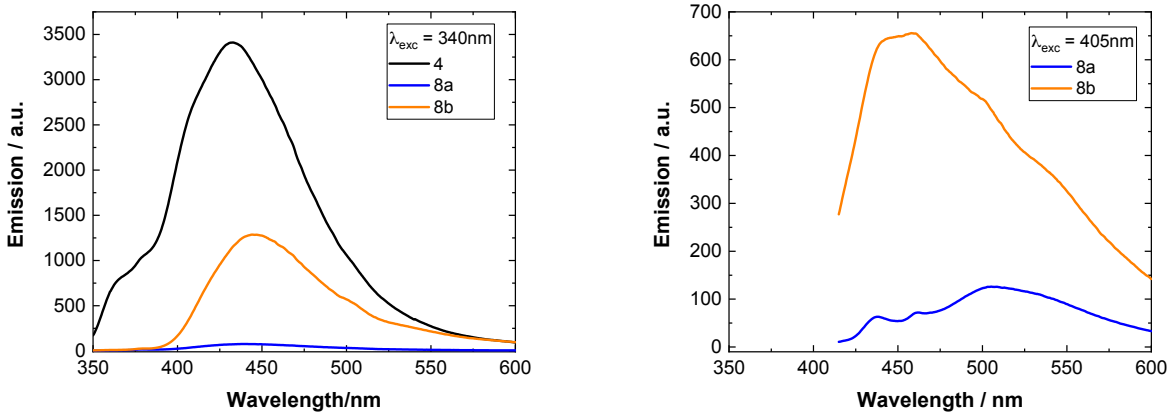

Figure S8. *Steady-state emission spectra of the ligand* ***4*** *(black) compared to that of the complexes* ***8a*** *(blue) and* ***8b*** *(orange) after 340 nm (left) and 405 nm excitation (right) in acetone. Note that the sensitivity of the spectrofluorometer was set to "high", whereas it was set to "low" for the other complexes (see Figure S10 below).*

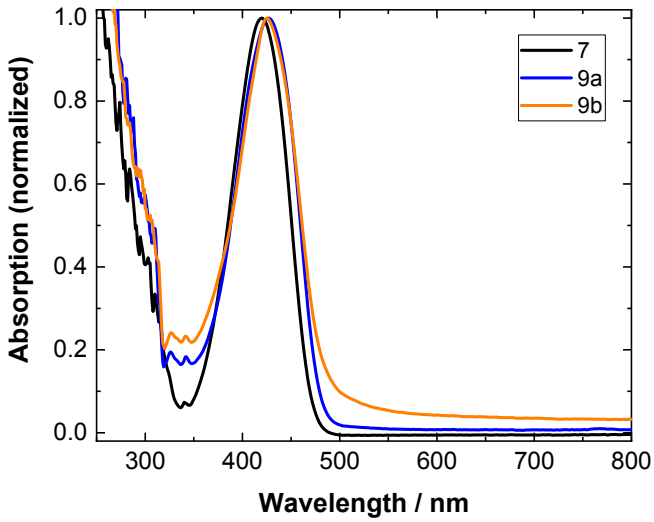

Figure S9. *Steady-state UV/Vis absorption spectra of the complexes* ***9a*** *(blue),* ***9b*** *(orange) and the free NHC ligand* ***7*** *(black) recorded in acetone.*

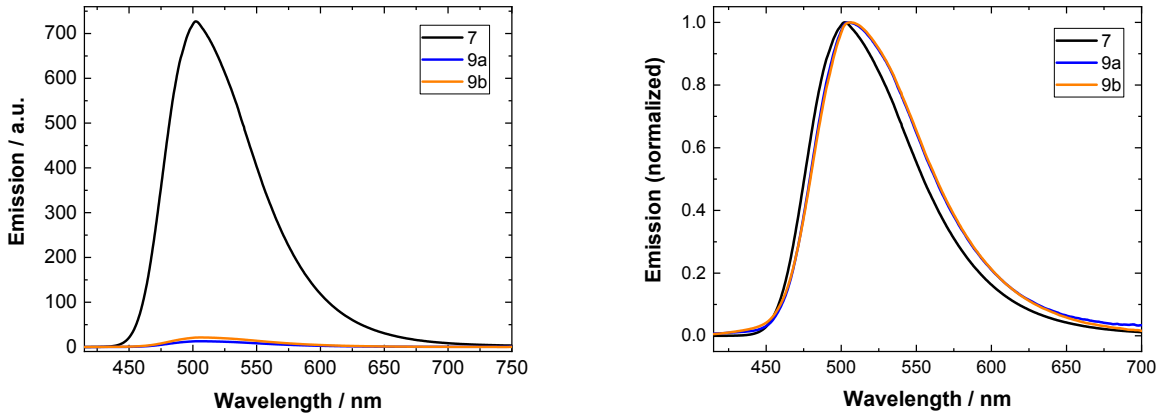

Figure S10. *Steady-state emission spectra of the ligand **7** (black) compared to that of the complexes **9a** (blue) and **9b** (orange) after 405 nm excitation in acetone, displayed in dependence on the relative emission intensities (left) and normalized to the emission maximum (right). Note that the sensitivity of the spectrofluorometer was set to "low", whereas it was set to "high" for the other complexes (see Figure S8 above).*

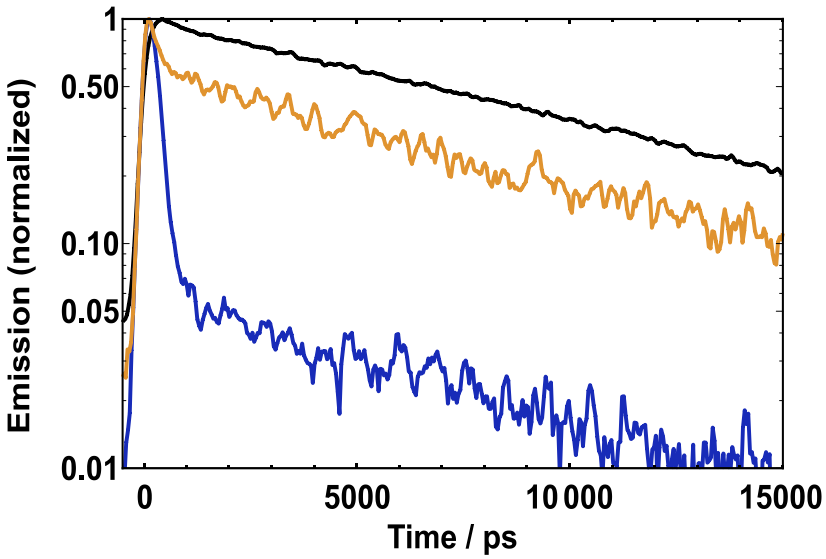

Figure S11. *Fluorescence decay of ligand **7** (black), complex **9a** (blue) and **9b** (orange) observed with a streak camera at an emission wavelength of 505 nm after excitation at 405 nm in acetone. The solubility of the complexes **9a/b** in the mixture water / 2 % DMSO was too low for time-resolved emission spectroscopy.*

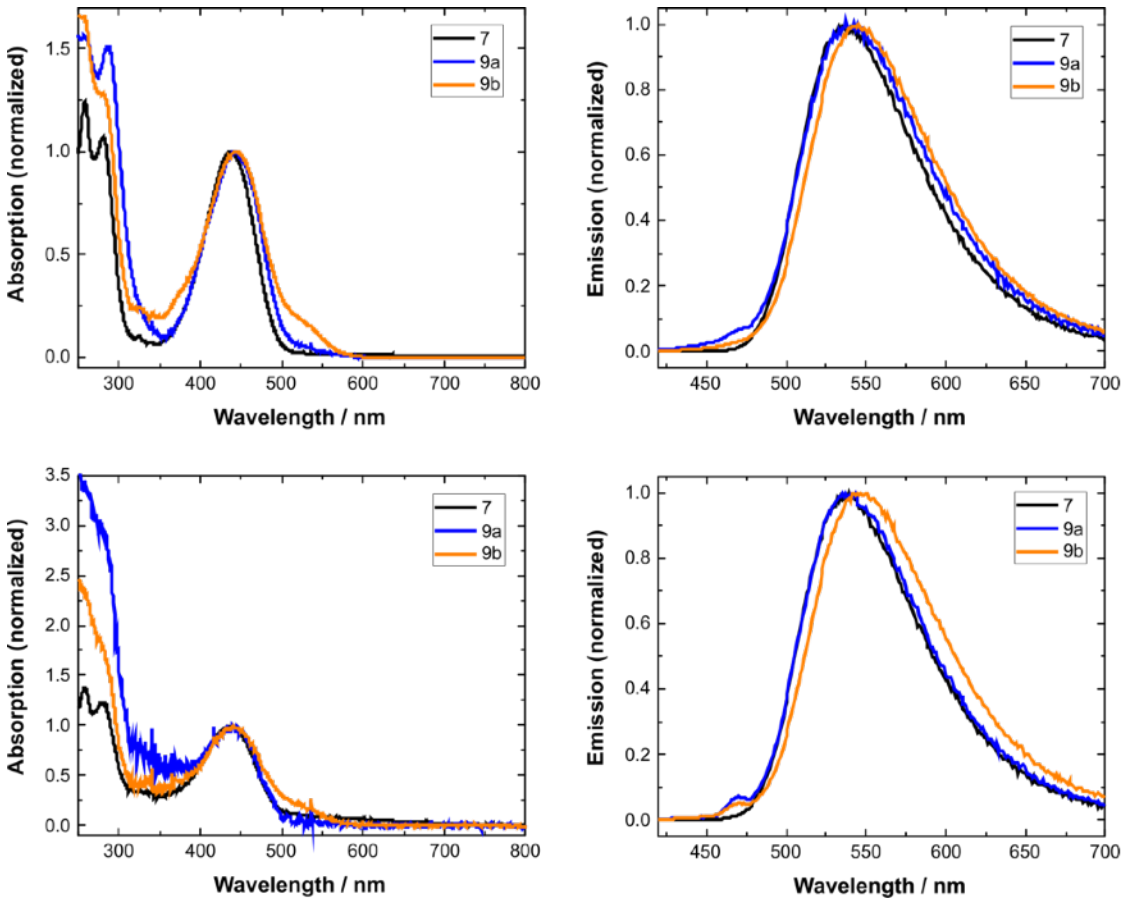

Figure S12. *Normalized steady-state UV/Vis absorption (left) and emission spectra (right), recorded after 405 nm excitation, of the complexes* ***9a*** *(blue),* ***9b*** *(orange) and the free NHC ligand* ***7*** *(black) dissolved in a 98 % water / 2 % DMSO mixture with a concentration of 20 µM (upper panels) and in a 99.8 % water / 0.2 % DMSO mixture with a concentration of 2 µM (lower panels), in analogy to the luminescence cell experiments. The displayed UV/Vis absorption spectra of* ***9a/b*** *were corrected for scattering contributions which are related to the low solubility of the compounds in water.*

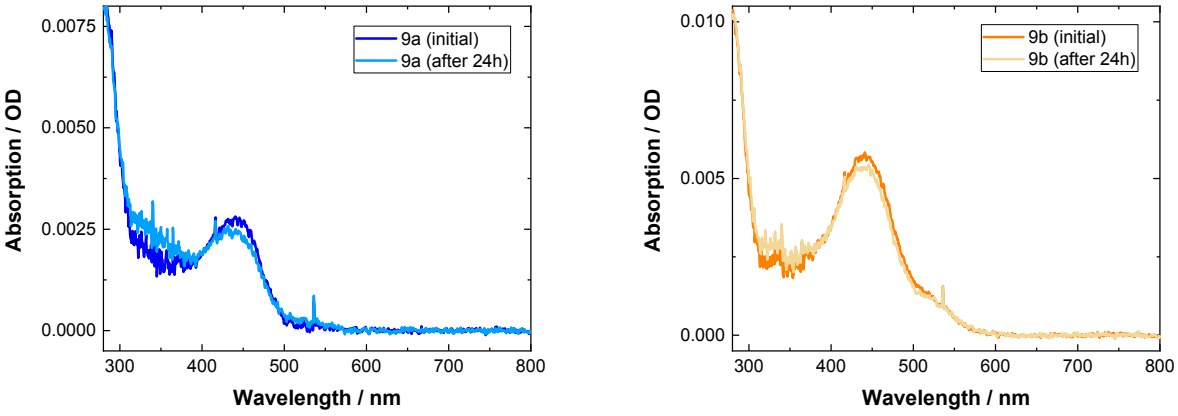

Figure S13. *UV/Vis absorption spectra of the complexes* ***9a*** *(left) and* ***9b*** *(right) dissolved in a 99.8% water / 0.2 % DMSO mixture. A 2 µM solution of each complex* ***9a*** *and* ***9b*** *was measured in constant time intervals over 24 hours, in order to check the stability of the complexes in water for the luminescence cell experiments performed at the same concentration of 2 µM. The displayed UV/Vis absorption spectra were corrected for scattering contributions which are related to the low solubility of the compounds in water.*

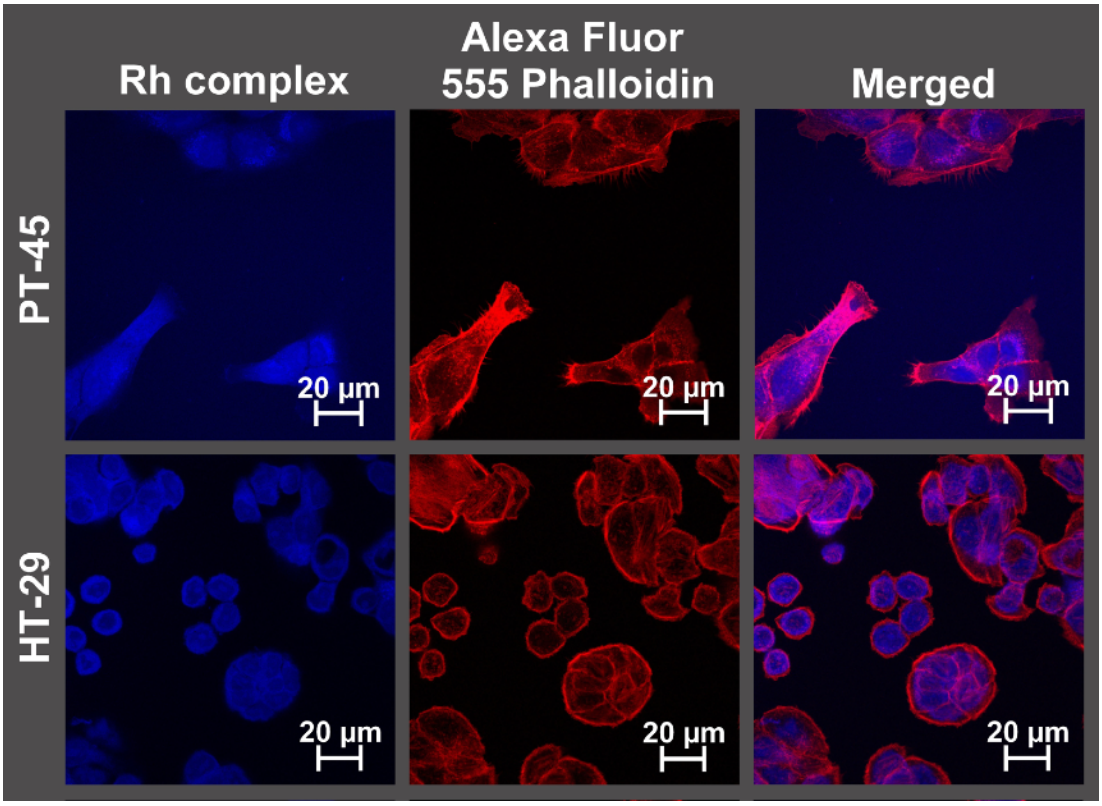

Figure S14. *Images obtained by confocal microscopy for PT-45 and HT-29 cells incubated with a 2 µM concentration of complex* ***9a*** *in an incubator at 37°C and 10% of CO_2 for 30 min. The cells were subsequently aldehyde fixed, their membranes permeabilized and F-actin filaments were stained with Alexa Fluor 555 Phalloidin. Natural luminescence when excited at 405 nm (blue) and 561 nm (red) respectively is shown. While the blue luminescence representing complex* ***9a*** *is mainly located inside of the cells the red luminescence marks the outer cytoskeleton of the cells. This indicates cellular uptake of complex* ***9a*** *with no specific intracellular distribution.*

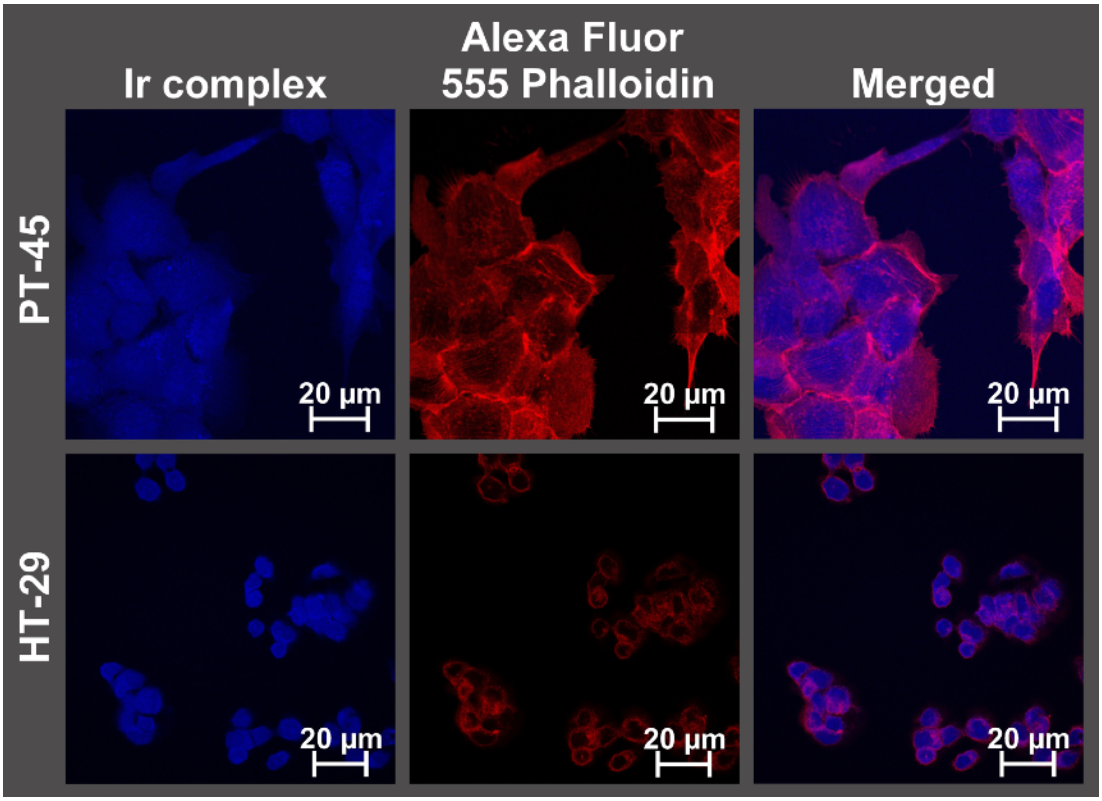

Figure S15. *Images obtained by confocal microscopy for PT-45 and HT-29 cells incubated with a 2 µM concentration of complex* ***9b*** *in an incubator at 37°C and 10% of CO_2 for 30 min. The cells were subsequently aldehyde fixed, their membranes permeabilized and F-actin filaments were stained with Alexa Fluor 555 Phalloidin. Natural luminescence when excited at 405 nm (blue) and 561 nm (red) respectively is shown. While the blue luminescence representing complex* ***9b*** *is mainly located inside of the cells the red luminescence marks the outer cytoskeleton of the cells. This indicates cellular uptake of complex* ***9b*** *with no specific intracellular distribution.*

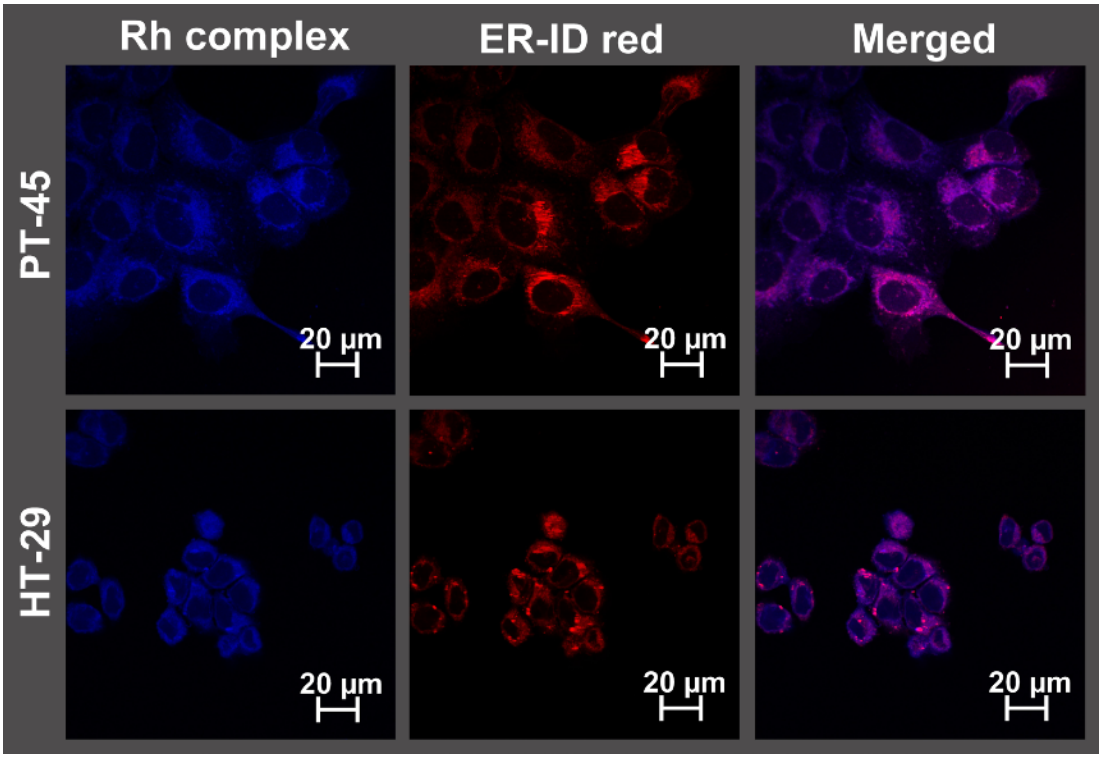

Figure S16. *Images obtained by confocal microscopy for PT-45 and HT-29 cells incubated with a 2 µM concentration of complex* ***9a*** *in an incubator at 37°C and 10% of CO_2 for 30 min. The cells were subsequently aldehyde fixed and the endoplasmatic reticulum was stained with ER-ID red. Natural luminescence when excited at 405 nm (blue) and 561 nm (red) respectively is shown. The blue luminescence representing complex* ***9a*** *shows a good overlay with the red luminescence representing the endoplasmatic reticulum. This indicates localization of complex* ***9a*** *in the endoplasmatic reticulum.*

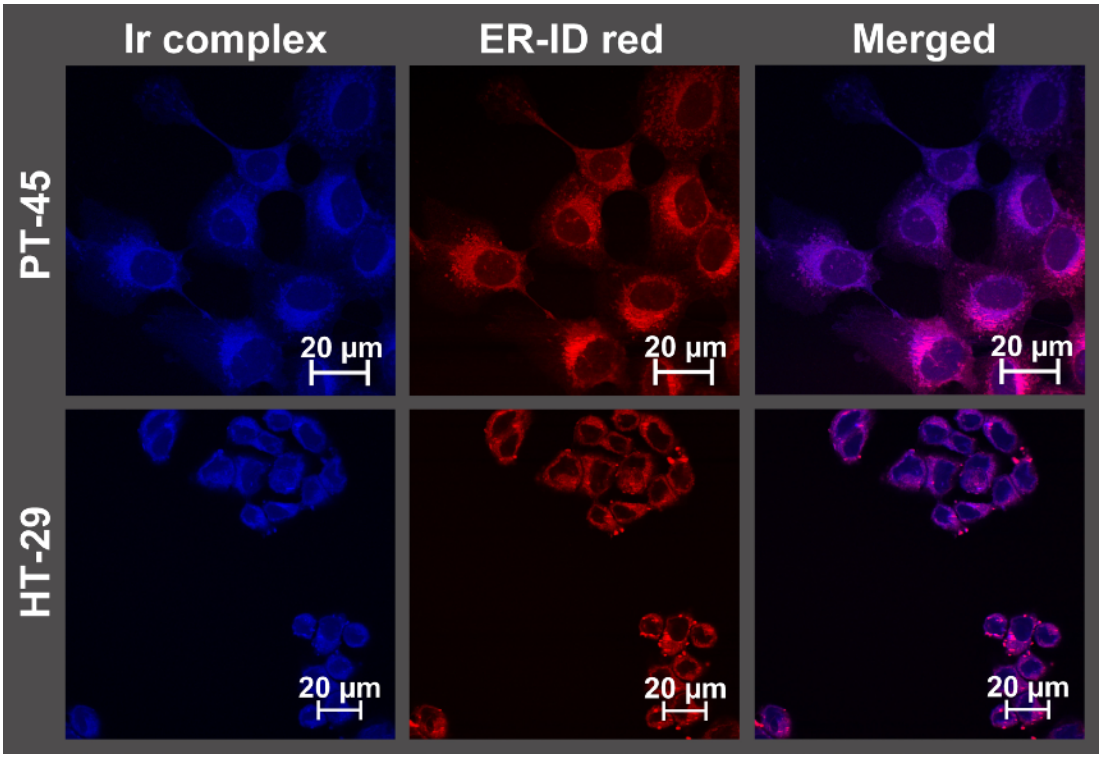

Figure S17. *Images obtained by confocal microscopy for PT-45 and HT-29 cells incubated with a 2 µM concentration of complex* ***9b*** *in an incubator at 37°C and 10% of CO_2 for 30 min. The cells were subsequently aldehyde fixed and the endoplasmatic reticulum was stained with ER-ID red. Natural luminescence when excited at 405 nm (blue) and 561 nm (red) respectively is shown. The blue luminescence representing complex* ***9b*** *shows a good overlay with the red luminescence representing the endoplasmatic reticulum. This indicates localization of complex* ***9b*** *in the endoplasmatic reticulum.*

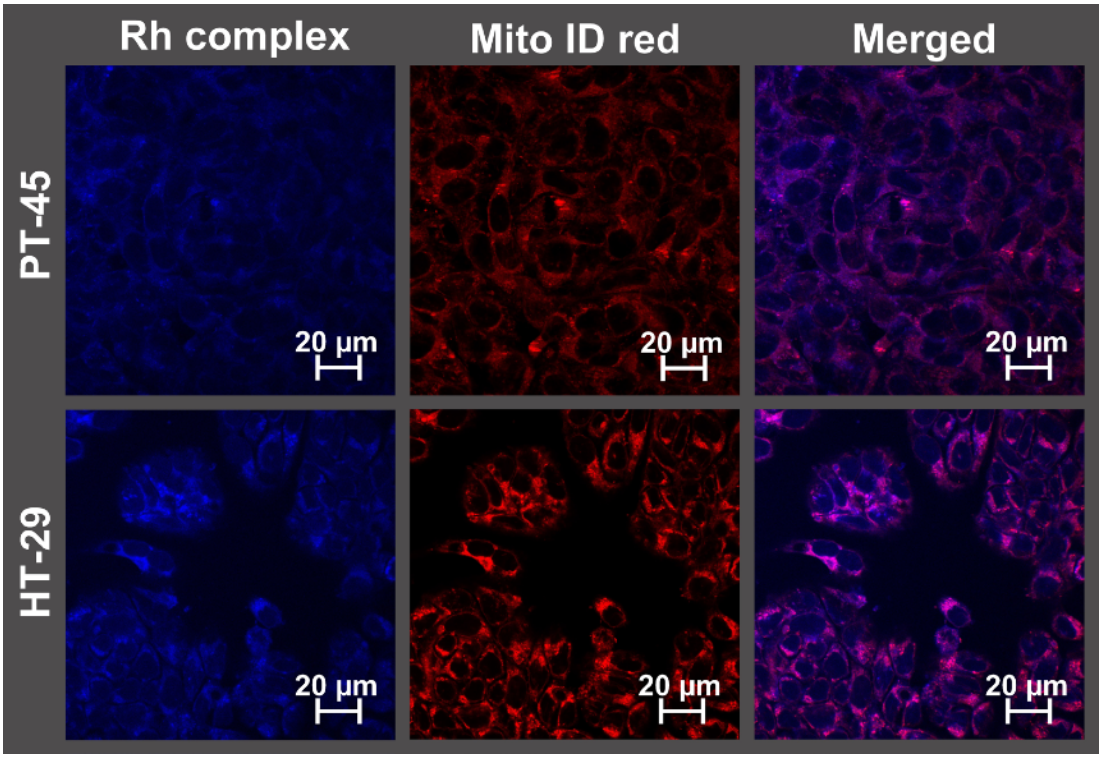

Figure S18. *Images obtained by confocal microscopy for PT-45 and HT-29 cells incubated with a 2 µM concentration of complex* ***9a*** *in an incubator at 37°C and 10% of CO_2 for 30 min. The cells were subsequently aldehyde fixed and the mitochondria were stained with Mito-ID red. Natural luminescence when excited at 405 nm (blue) and 561 nm (red) respectively is shown. The blue luminescence representing complex* ***9a*** *shows some degree of overlay with the red luminescence representing the mitochondria. This indicates some degree of localization of complex* ***9a*** *in the mitochondria.*

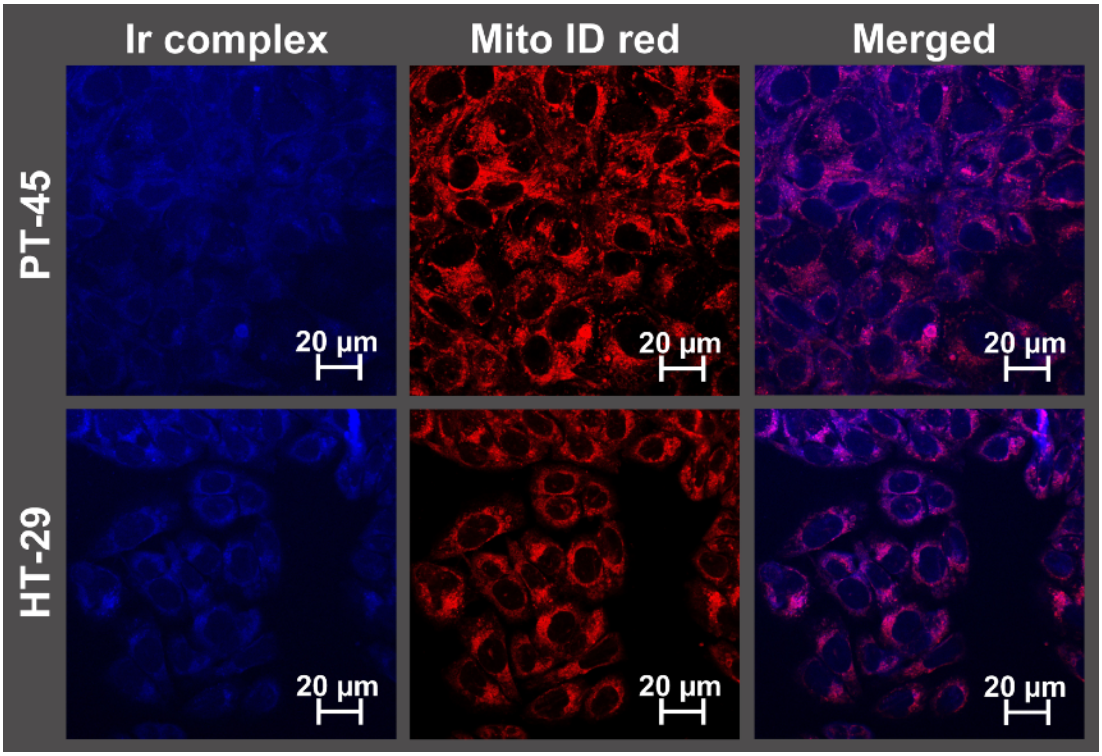

Figure S19. *Images obtained by confocal microscopy for PT-45 and HT-29 cells incubated with a 2 µM concentration of complex* ***9b*** *in an incubator at 37°C and 10% of CO_2 for 30 min. The cells were subsequently aldehyde fixed and the mitochondria were stained with Mito-ID red. Natural luminescence when excited at 405 nm (blue) and 561 nm (red) respectively is shown. The blue luminescence representing complex* ***9b*** *shows some degree of overlay with the red luminescence representing the mitochondria. This indicates some degree of localization of complex* ***9b*** *in the mitochondria.*

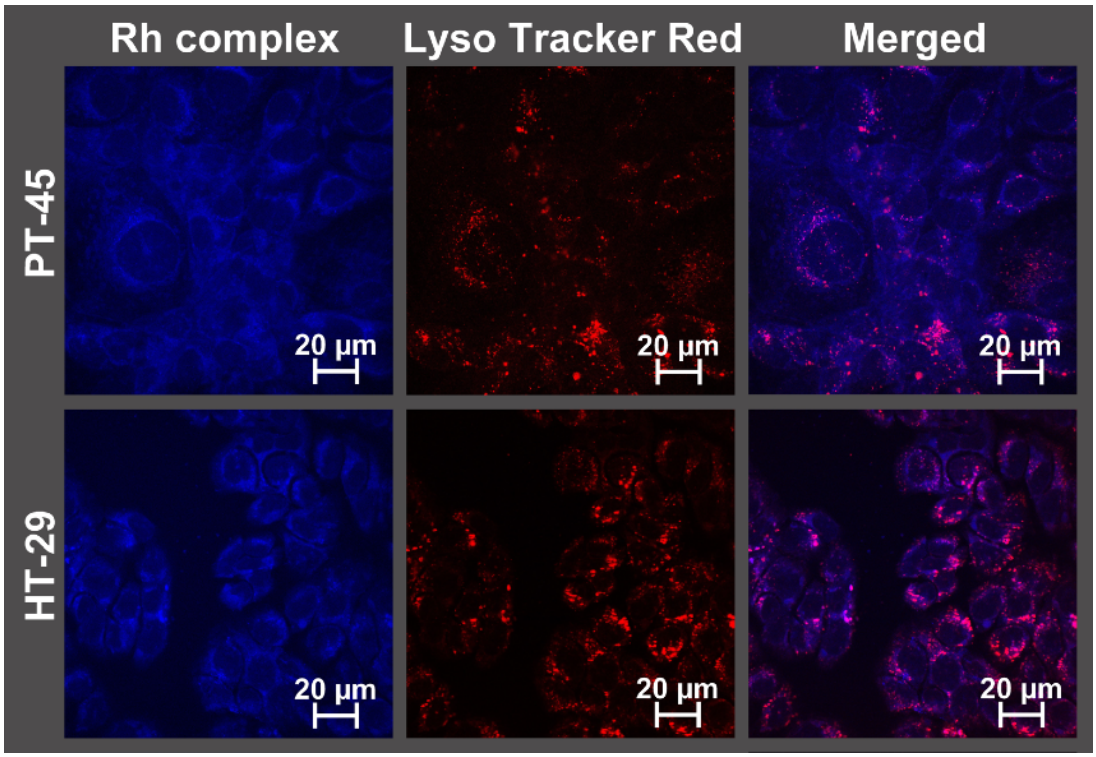

Figure S20. *Images obtained by confocal microscopy PT-45 and HT-29 cells incubated with a 2 µM concentration of complex* ***9a*** *in an incubator at 37°C and 10% of CO_2 for 30 min and subsequently treated with LysoTracker red for 30 min in similar conditions before being fixed with aldehyde. Natural luminescence when excited at 405 nm (blue) and 561 nm (red) respectively is shown. The blue luminescence representing complex* ***9a*** *shows only a minor overlay with the red luminescence representing the lysosomes. This indicates low degrees of localization of complex* ***9a*** *in the lysosomes.*

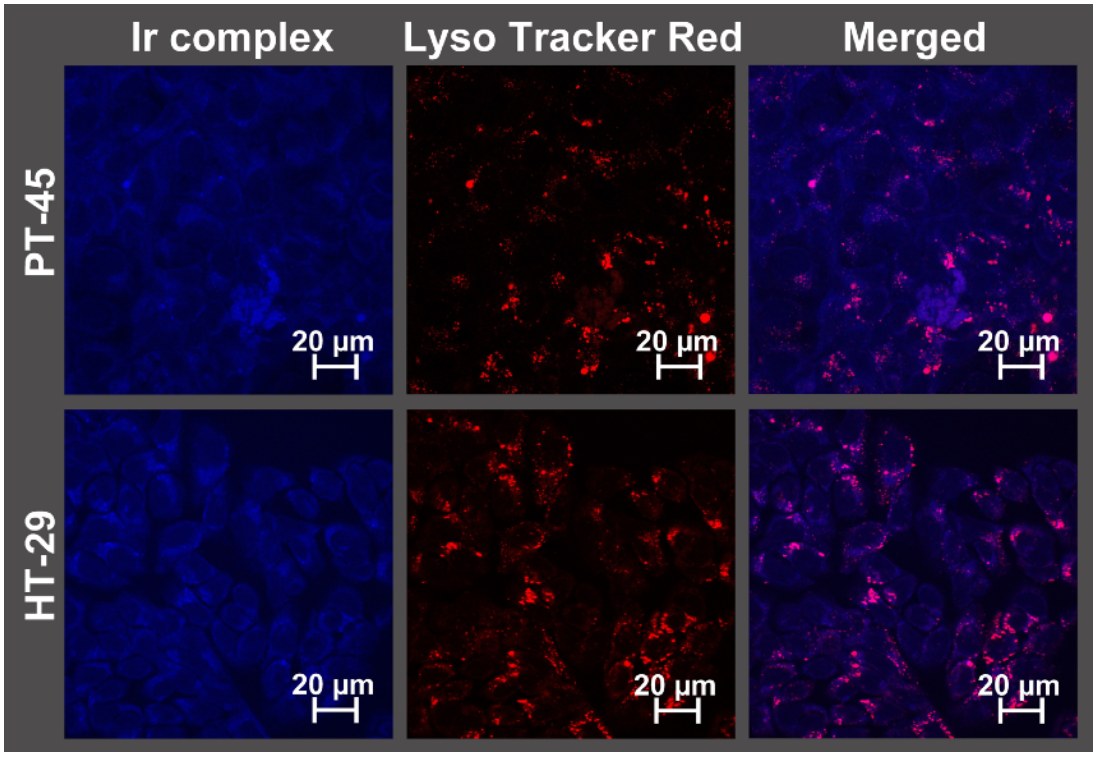

Figure S21. *Images obtained by confocal microscopy PT-45 and HT-29 cells incubated with a 2 µM concentration of complex* ***9b*** *in an incubator at 37°C and 10% of CO_2 for 30 min and subsequently treated with LysoTracker red for 30 min in similar conditions before being fixed with aldehyde. Natural luminescence when excited at 405 nm (blue) and 561 nm (red) respectively is shown. The blue luminescence representing complex* ***9b*** *shows only a minor overlay with the red luminescence representing the lysosomes. This indicates low degrees of localization of complex* ***9b*** *in the lysosomes.*

3. Spectra of metal containing compounds

3.1 ^{1}H-NMR spectra

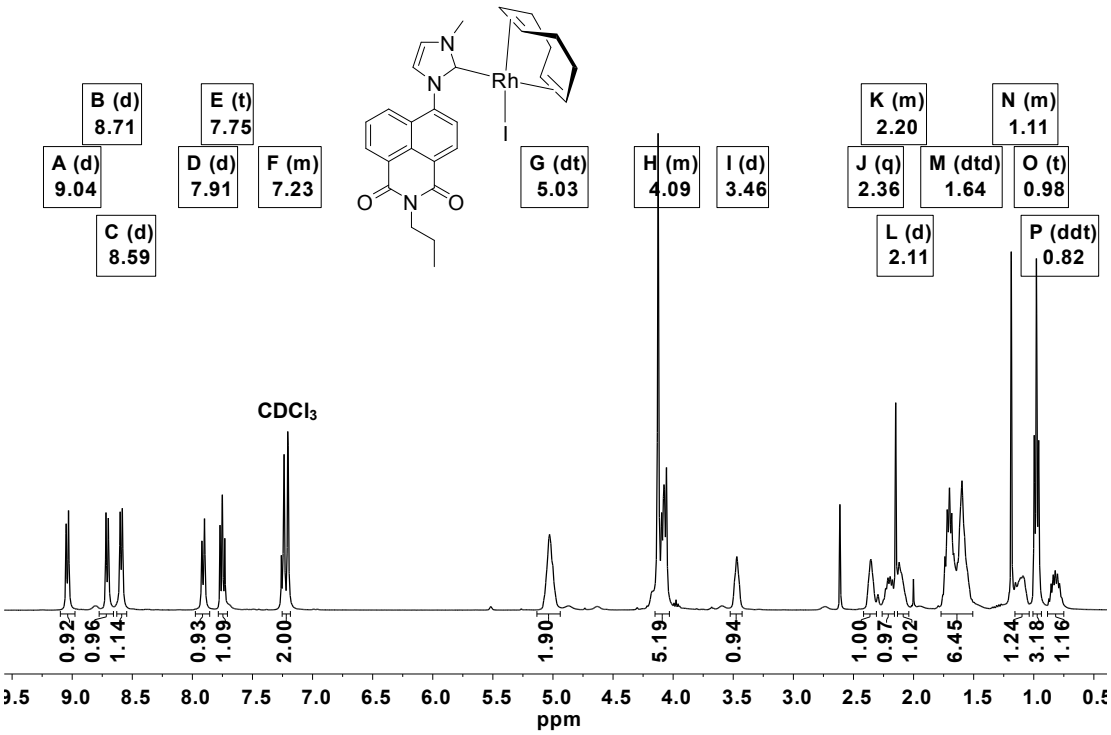

Figure S22. *^{1}H-NMR spectrum (400 MHz) of complex **8a**.*

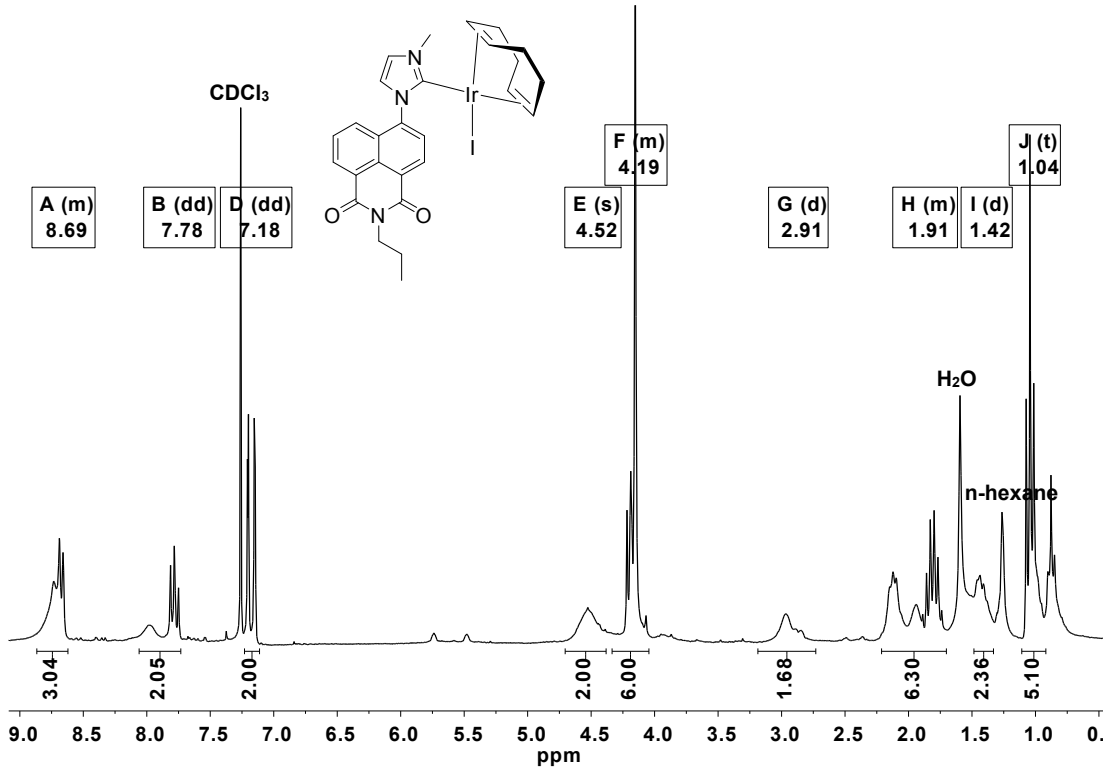

Figure S23. *[1]H-NMR spectrum (400 MHz) of complex* ***8b****.*

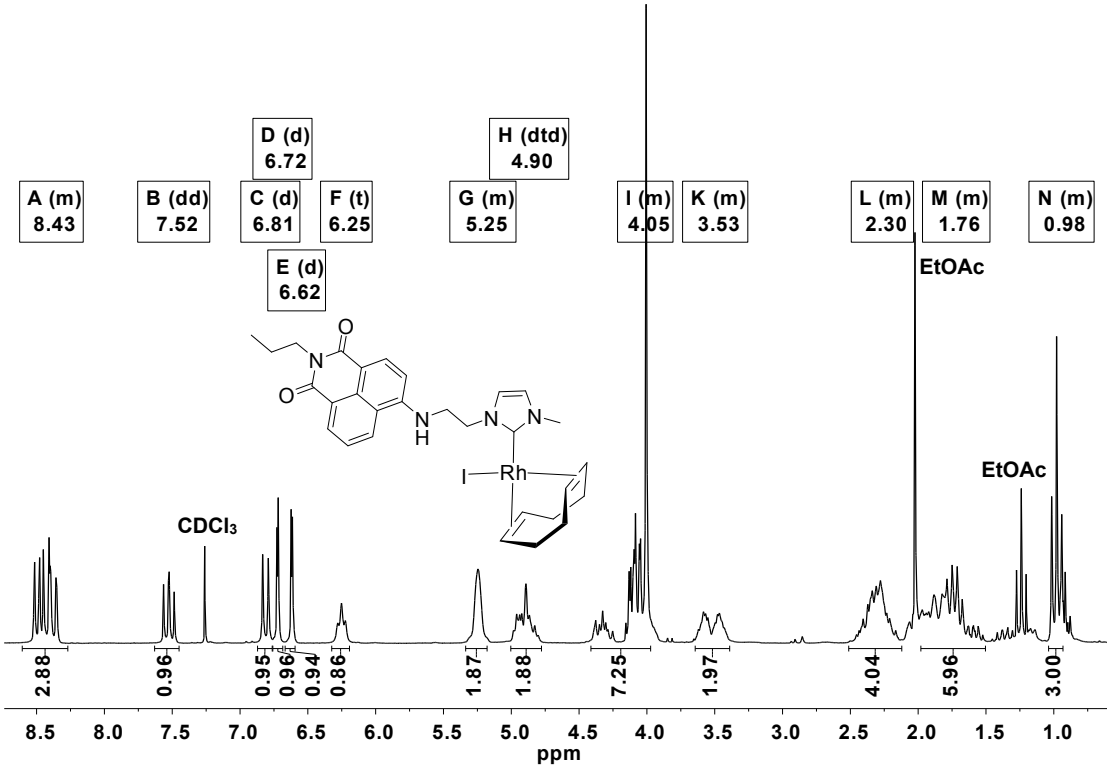

Figure S24. *[1]H-NMR spectrum (400 MHz) of complex* ***9a****.*

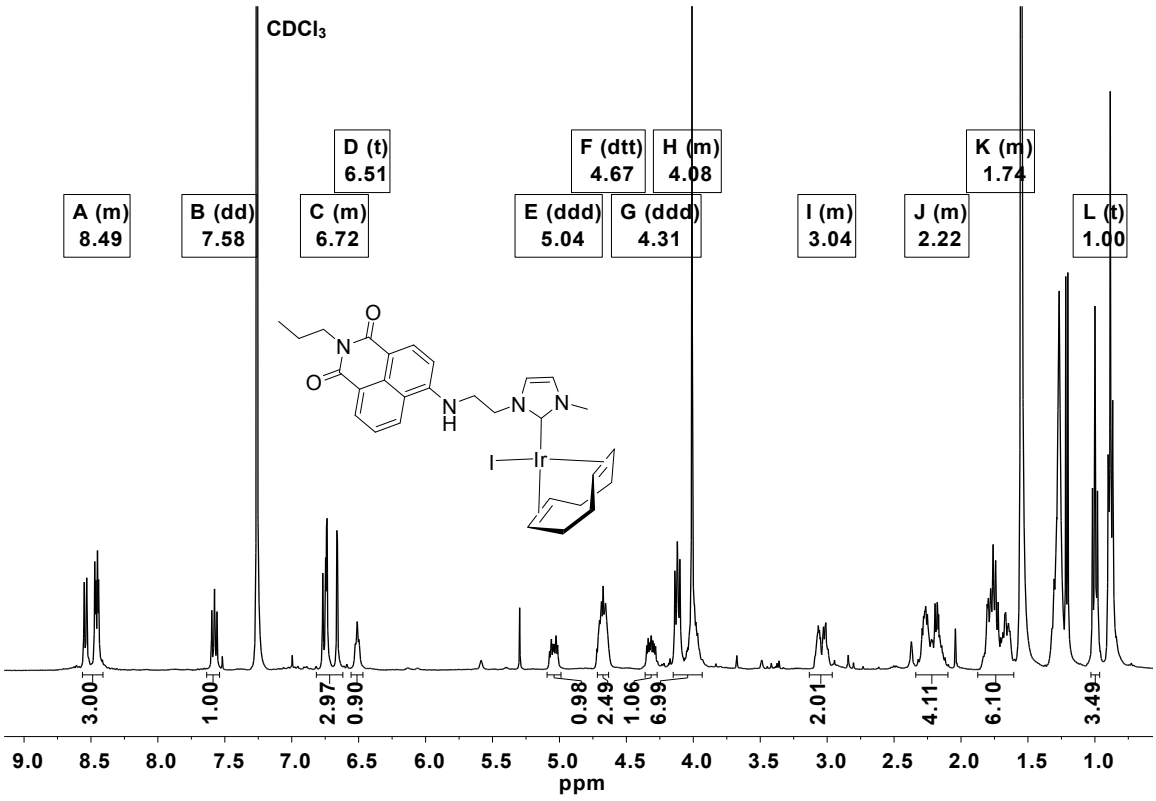

Figure S25. *[1]H-NMR spectrum (400 MHz) of complex* ***9b****.*

3.2 2D NMR spectra

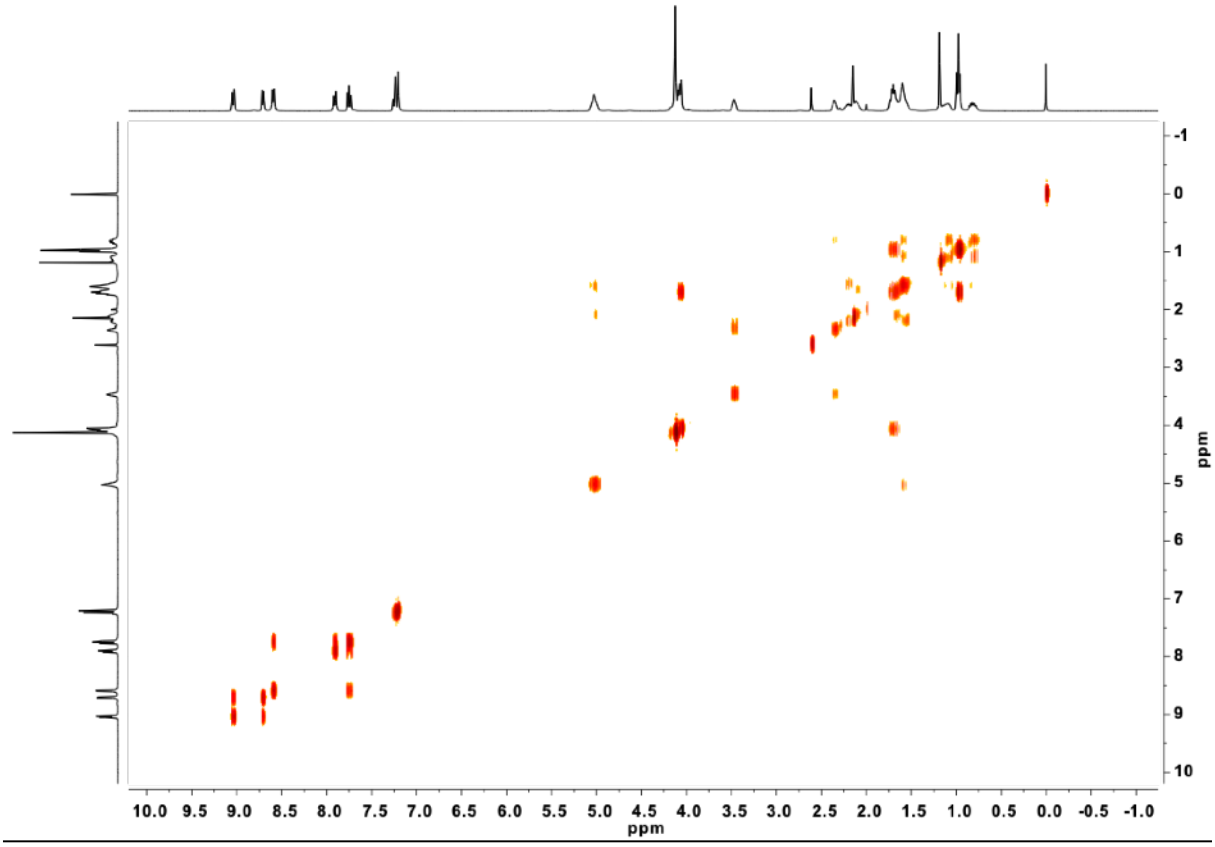

Figure S26. *^{1}H-^{1}H Cosy NMR spectrum of complex* ***8a***.

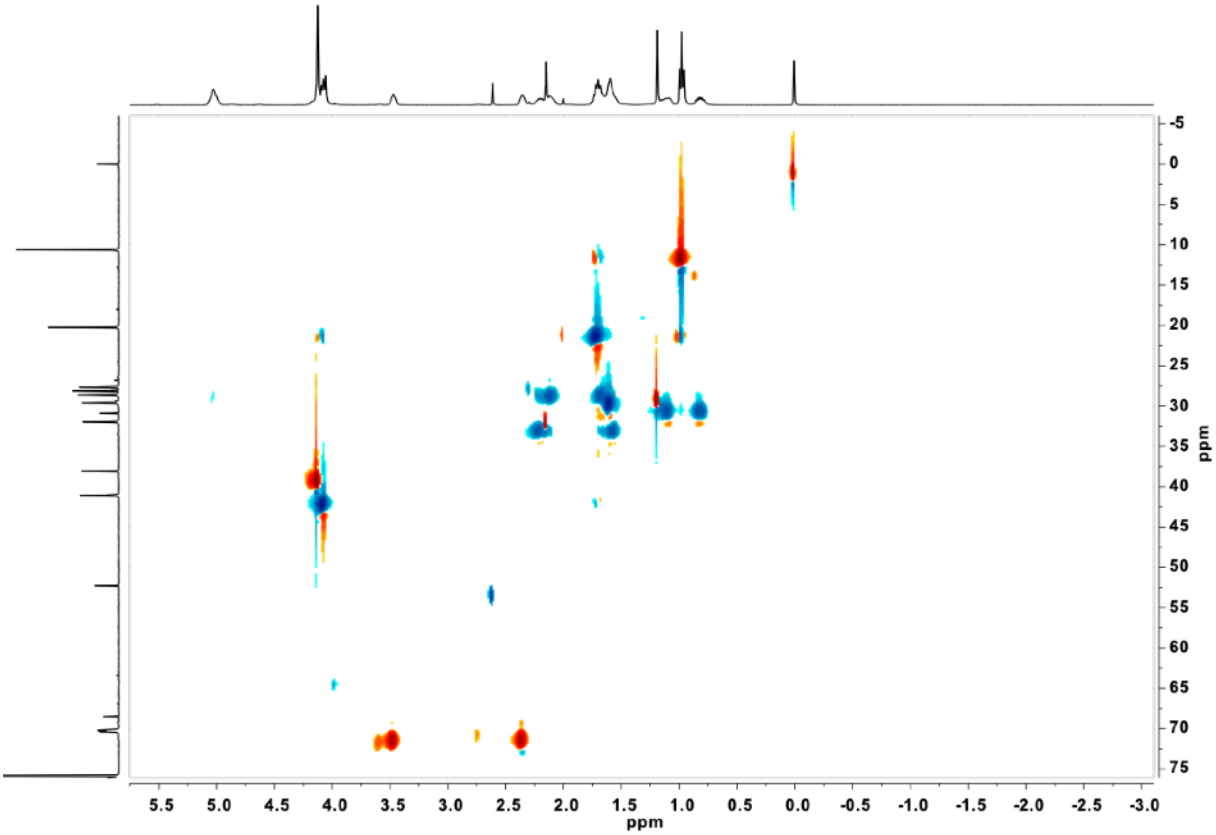

Figure S27. *^{1}H-^{13}C{1H} HSQC NMR spectrum of complex* ***8a***.

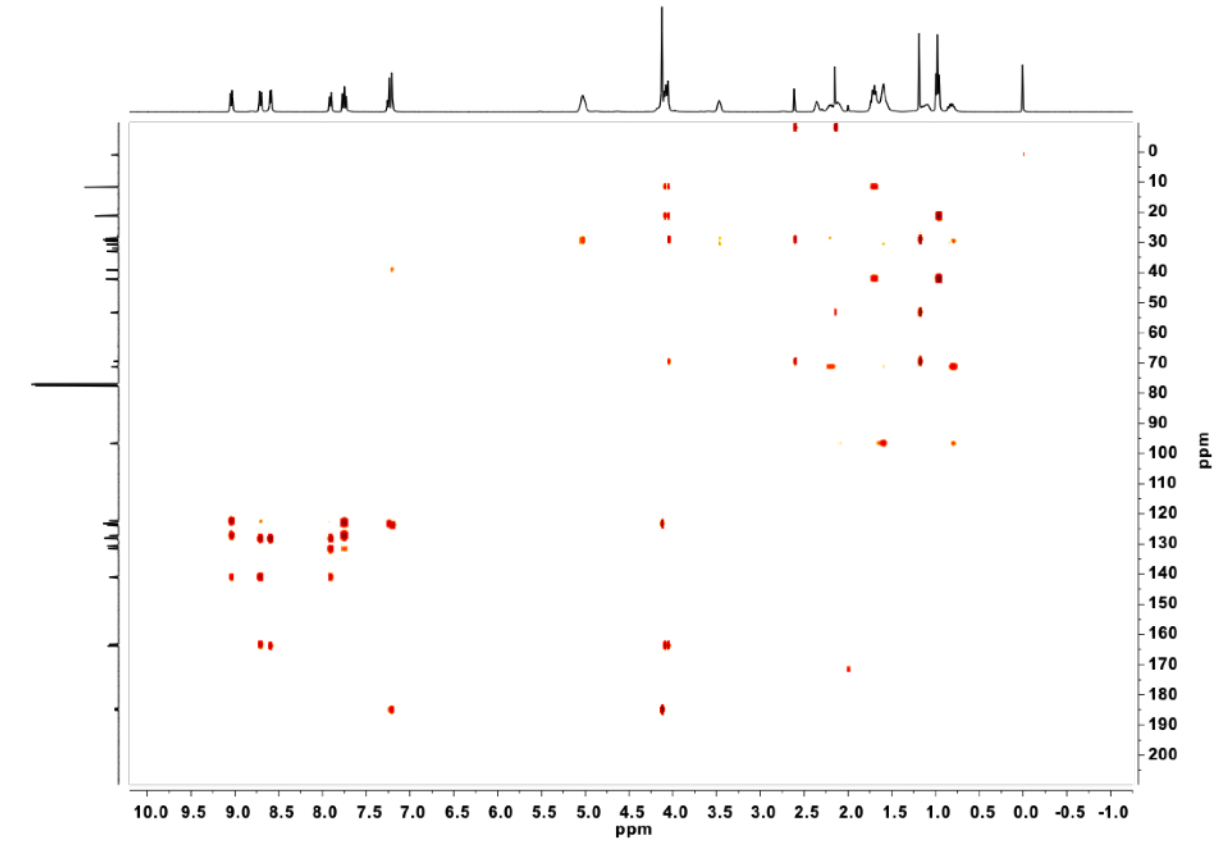

Figure S28. *^{1}H-^{13}C{1H} HMBC NMR spectrum of complex* ***8a***.

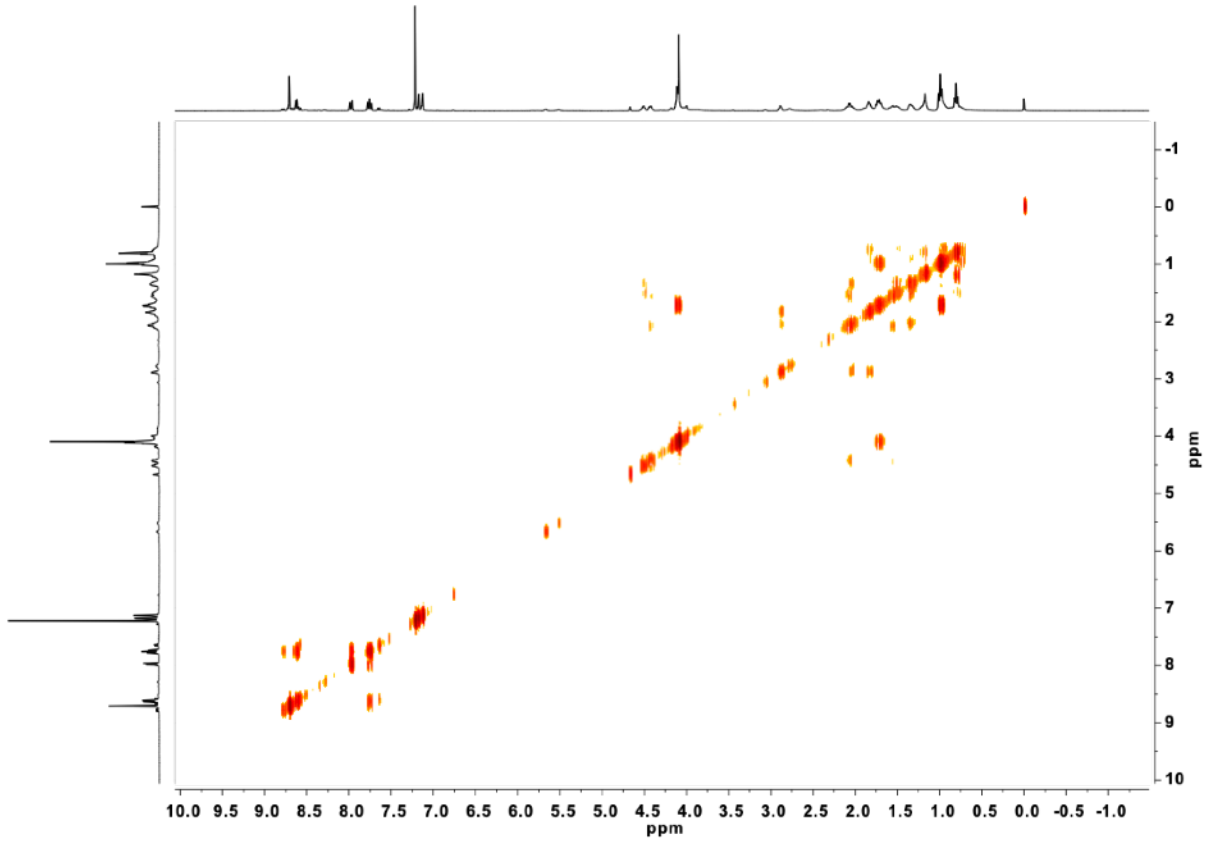

Figure S29. *^{1}H-^{1}H Cosy NMR spectrum of complex* ***8b***.

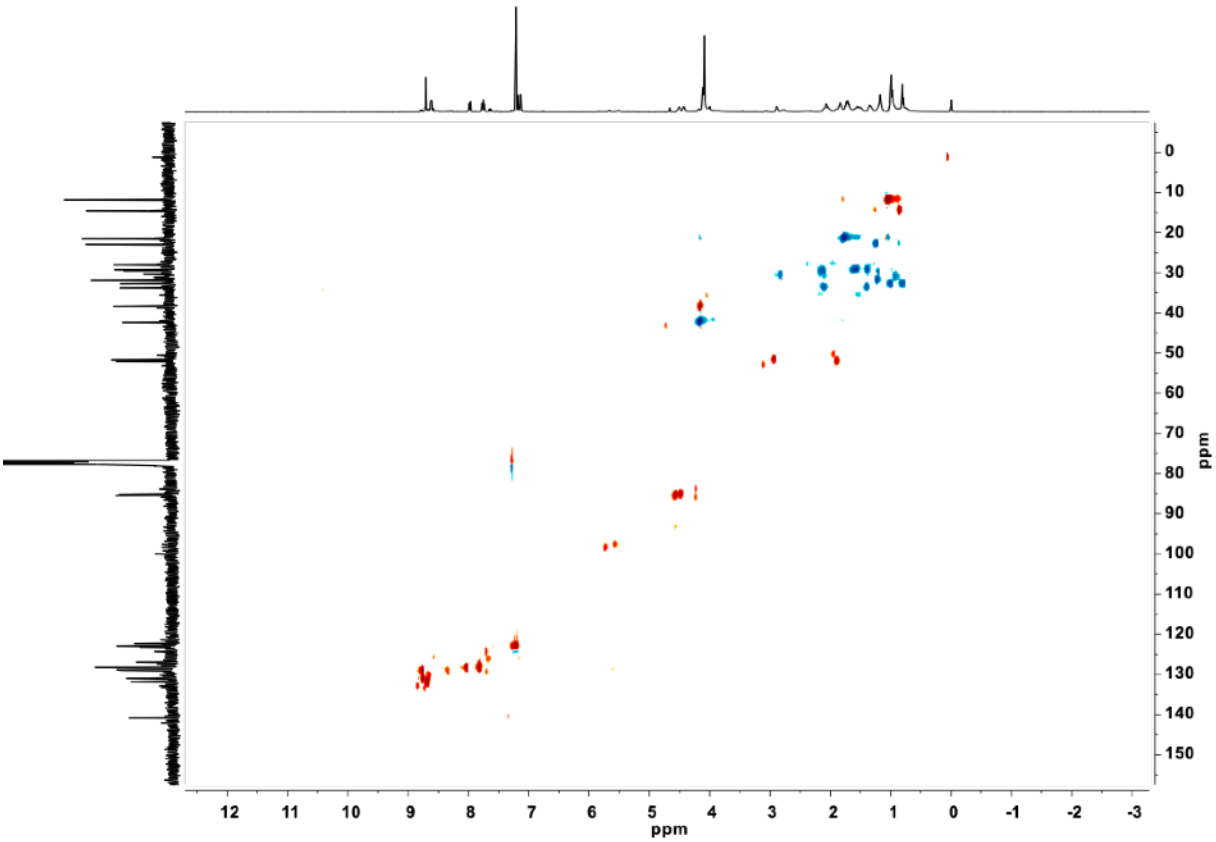

Figure S30. *^{1}H-^{13}C{1H} HSQC NMR spectrum of complex* ***8b***.

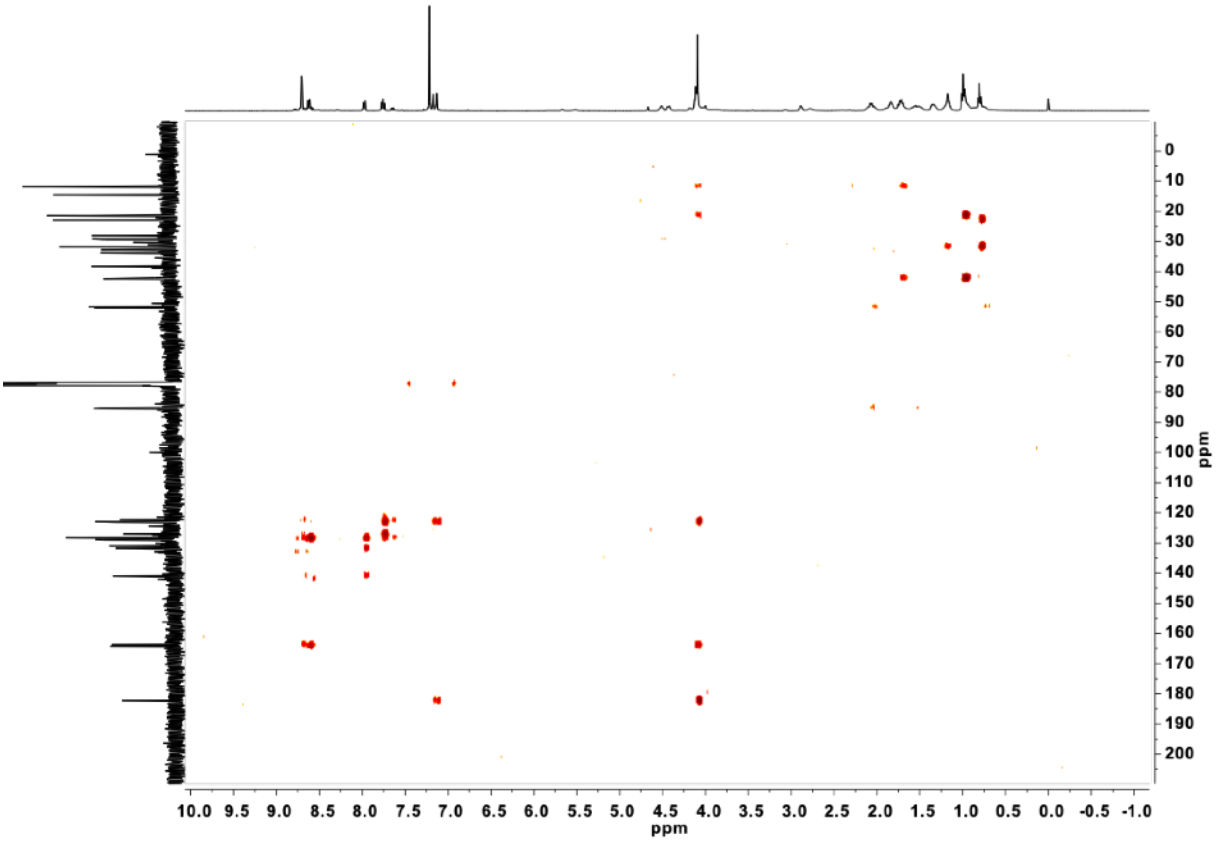

Figure S31. *^{1}H-^{13}C{1H} HMBC NMR spectrum of complex* ***8b***.

3.2 ESI-MS spectra

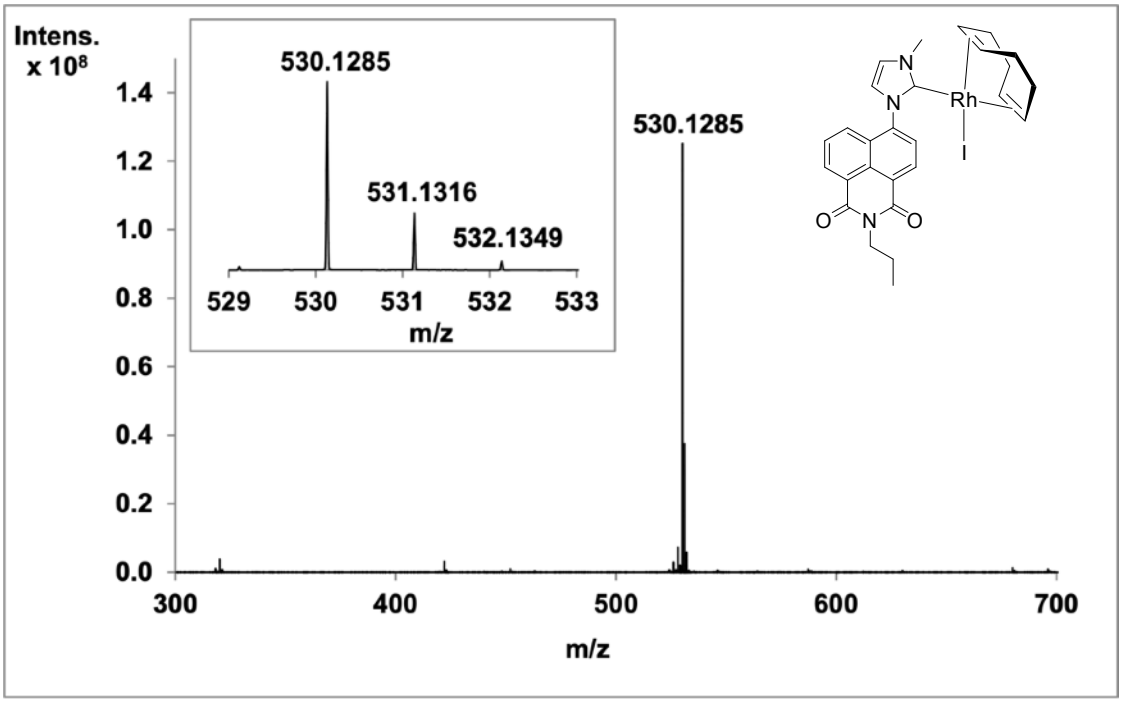

Figure S32. *High resolution ESI-MS spectrum of complex* ***8a***.

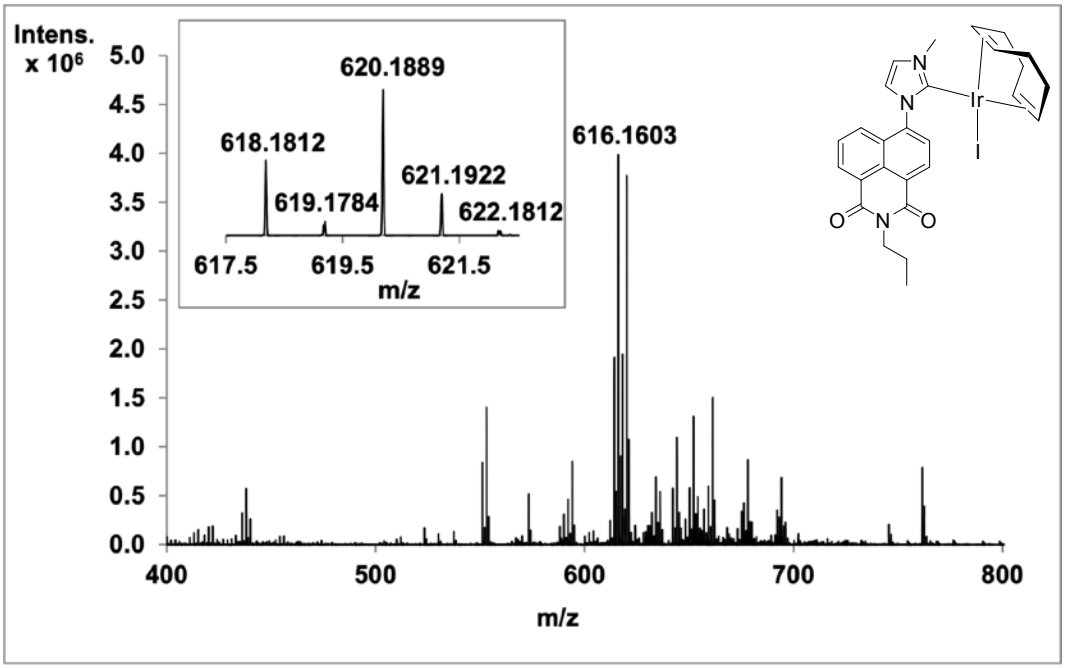

Figure S33. *High resolution ESI-MS spectrum of complex* ***8b****.*

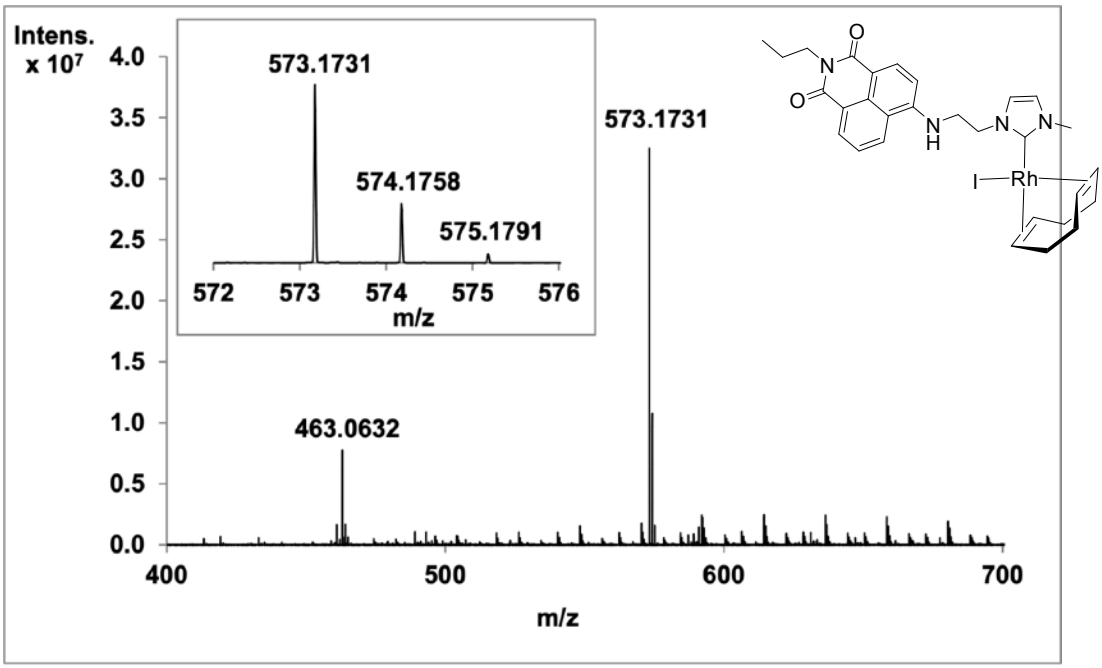

Figure S34. *High resolution ESI-MS spectrum of complex* ***9a****.*

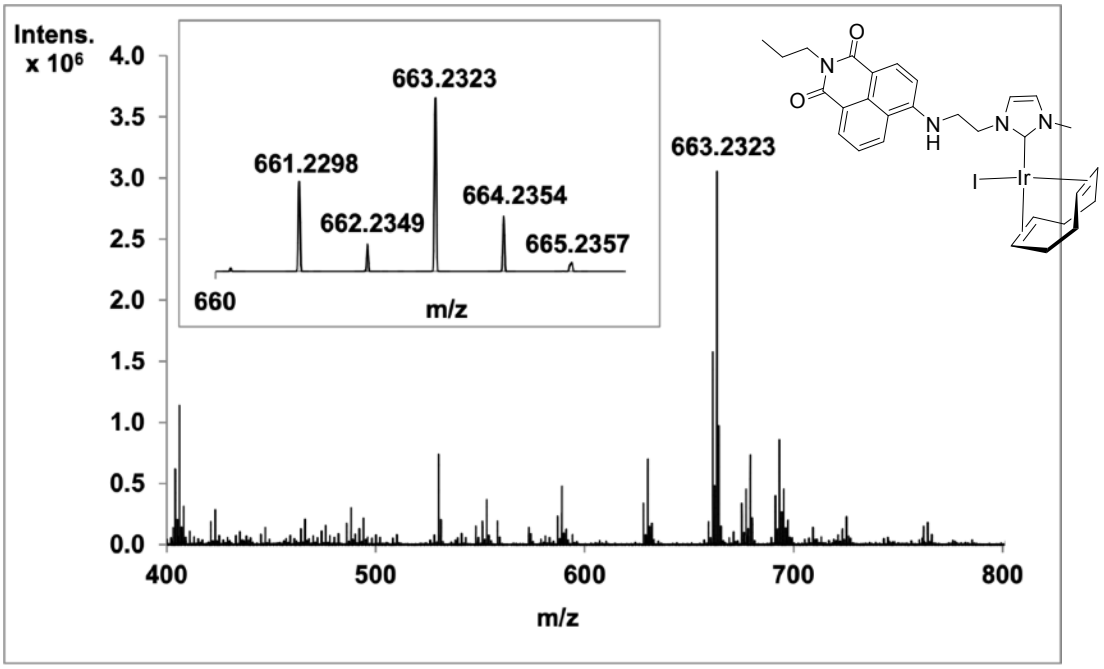

Figure S35. *High resolution ESI-MS spectrum of complex* ***9b****.*

4. Crystal structure data

Table S1: *Crystal data and structure refinement for compounds* ***4***, ***6***, ***8a*** *and* ***9a***

Compound N°	**4**	**6**	**8a**	**9a**
Empirical formula	$C_{57}H_{58}I_3N_9O_8$	$C_{21}H_{21}IN_2O_3$	$C_{28}H_{31}Cl_2IN_3O_2Rh$	$C_{29}H_{34}IN_4O_2Rh$
Formula weight	1377.82 g/mol	476.30 g/mol	742.27 g/mol	700.41 g/mol
Temperature	104(6) K	113(4) K	99.9(6) K	100.00(10) K
Wavelength	1.54184 Å	1.54184 Å	1.54184 Å	1.54184 Å
Crystal system	Triclinic	Monoclinic	Triclinic	Monoclinic
Space group	P-1	P21/c	P-1	P21/n
Unit cell dimensions	a = 14.3926(5) Å b = 14.9046(5) Å c = 16.4864(6) Å α = 111.852(3)° β = 92.985(3)° γ = 117.547(4)°	a = 4.64750(10) Å b = 14.3236(2) Å c = 30.4596(6) Å α = 90° β = 90.595(2)° γ = 90°	a = 9.28430(10) Å b = 12.47860(10) Å c = 13.71230(10) Å α= 106.9850(10)° β= 99.6890(10)° γ = 105.4590(10)°	a = 12.3647(2) Å b = 14.8794(3) Å c = 15.1745(4) Å α= 90° β= 96.395(2)° γ = 90°
Volume	2800.2(2) $Å^3$	2027.55(7) $Å^3$	1411.19(2) $Å^3$	2774.42(10) $Å^3$
Z	2	4	2	4
Density (calculated)	1.634 Mg/m^3	1.560 Mg/m^3	1.747 Mg/m^3	1.677 Mg/m^3
Absorption coefficient	13.660 mm^{-1}	12.598 mm^{-1}	15.468 mm^{-1}	13.975 mm^{-1}
F(000)	1372	952	736	1400
Theta range for data collection	3.598 to 67.500°	3.410 to 77.575°	3.497 to 67.498°	4.174 to 76.243°
Reflections collected	26078	14958	19119	15041
Independent reflections	10090 [R(int) = 0.0342]	4021 [R(int) = 0.0487]	5063 [R(int) = 0.0514]	5758 [R(int) = 0.0333]
Completeness to theta = 67.684°	100.0 %	95.7 %	99.9 %	100.0 %
Data / restraints / parameters	10090 / 0 / 711	4021 / 0 / 245	5063 / 0 / 336	5758 / 0 / 356
Goodness-of-fit on F^2	1.029	1.137	1.051	1.062
Final R indices [I>2sigma(I)]	R1 = 0.0328, wR2 = 0.0848	R1 = 0.0675, wR2 = 0.1687	R1 = 0.0349, wR2 = 0.0917	R1 = 0.0372, wR2 = 0.0970
R indices (all data)	R1 = 0.0361, wR2 = 0.0879	R1 = 0.0713, wR2 = 0.1715	R1 = 0.0355, wR2 = 0.0924	R1 = 0.0436, wR2 = 0.1027